# An Ultra-Low Power Multivibrator-Based Wake-up Receiver for Wireless Sensor Networks

**Nowbahari, Arian; Marchetti, Luca; Azadmehr, Mehdi**
Department of Microsystems - University of South-Eastern Norway

This is an Accepted Manuscript of an article published by IEEE Online in *2021 IEEE 7th World Forum on Internet of Things (WF-IoT)* on November 9, 2021, available online:
https://doi.org/10.1109/WF-IoT51360.2021.9595159

Nowbahari, A., Marchetti, L., & Azadmehr, M. (2021, June 14-July 31). *An Ultra-Low Power Multivibrator-Based Wake-up Receiver for Wireless Sensor Networks* [Conference presentation]. 2021 IEEE 7th World Forum on Internet of Things (WF-IoT), New Orleans. https://doi.org/10.1109/WF-IoT51360.2021.9595159

# An Ultra-Low Power Multivibrator-Based Wake-up Receiver for Wireless Sensor Networks

Arian Nowbahari, Luca Marchetti, Mehdi Azadmehr
*Department of Microsystems (IMS)*
*University of South-Eastern Norway*
Borre, Norway
arian.nowbahari@usn.no

***Abstract*—In recent years wireless sensor networks (WSNs) have gained significant attention because of their implementation in many different fields. As the nodes in WSNs are typically battery-powered, their lifetime is mainly limited by the sensor nodes power consumption. A typical energy-saving solution consists in implementing wake-up receivers (WuRxs), which are responsible for the sensor node activation only when required. In this work an ultra-low power multivibrator-based WuRx concept is proposed. The WuRx is composed of several input-triggered multivibrators, which generate pulses of fixed duration. These pulses are compared to the input signal through logic gates, which are predefined according to the wake-up call. The sensor node is activated if the codes match. An implementation in TSMC-180nm CMOS process is proposed and simulated. The WuRx consumes 0.8µW when detecting a 6ms wake-up call signal, and 58.4pW when in idle mode.**

***Index Terms*—CMOS, low power, multivibrator, sensor node, wake-up receiver, wireless sensor network**

## I. Introduction

A wireless sensor network (WSN) can be defined as the ensemble of wirelessly connected sensor nodes capable of sensing, processing and transmitting signals [1]. WSNs are implemented in many applications (health, environmental, military), and are one of the main enabling technologies of the Internet-of-Things [2], [3]. They are typically powered by batteries, so their primary limitation is the sensor nodes power consumption, which limits the network lifetime [4]. Different energy-saving solutions have been investigated to optimize the WSN power management [5]. A possible method consists into set in sleep mode the sensor nodes, and wake up them according to a certain *rendezvous* scheme [6]. For instance in pure synchronous rendezvous schemes, sensor nodes are presynchronized to activate according to a well defined sleep schedule. But this approach is intrinsically affected by *idle listening* and *overhearing*. Idle listening occurs when the sensor node is active, but no communication is required, thus resulting in wasted energy [7]. Overhearing occurs when a sensor node overhears data that are not intended to it, thus being uselessly activated [8]. A practical solution to these problems is the implementation of pure asynchronous rendezvous schemes, where the sensor nodes are woken up according to an identity-based approach [9]. From a hardware point of view this translates in the implementation of wake-up receivers (WuRxs) [10]. In such a scheme (Fig.1) the sensor nodes are normally in deep sleep mode. When the correct wake-up call (WuC) is detected, the WuRx activates the sensor node through an interrupt signal. This approach is conceptually energy-saving, since the sensor nodes are activated only on demand. Wake-up receivers could be mainly classified in RF based and non-RF based WuRxs. The majority of WuRxs uses radio signals [11]–[15], while non-RF based solutions employ acoustic [16]–[22] and optical signals [23]–[26]. Most of the proposed WuRxs in the literature presents complex and power consuming architectures. In this work a simple and low power WuRx concept is proposed. In Section II the WuRx architecture is reported. In Section III a circuit implementation is presented, while the simulations results are in Section IV.

This work was supported by the Research Council of Norway under the Advanced Piezoelectric Devices project [273248].

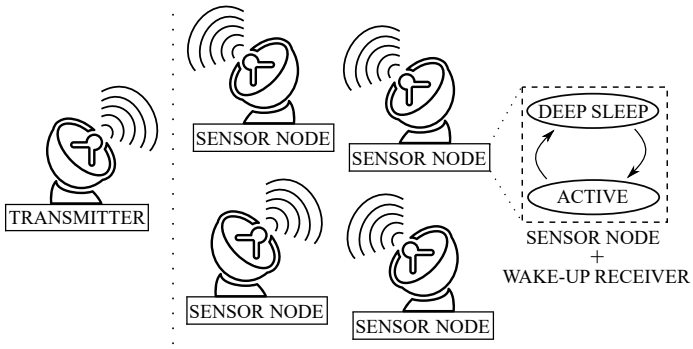


Fig. 1. Wireless sensor network implementing wake-up receivers.

## II. Architecture

The architecture of the proposed WuRx is shown in Fig.2. Since the amplitude of the received input signal $S_{in}$ could be small (e.g. because of losses and/or distance from the transmitter), a step-up block may be considered. The second block (rectification) is used to convert the AC input signal into square-shaped waves with duration equal to that of $S_{in}$. This rectified signal ($S_{rect}$) goes into the first state detector $D_1$, which is composed of a monostable (also called *one-shot* [27]) multivibrator and a logic gate. The multivibrator generates the pulse $S_{p_1}$ in response to the input pulse (i.e.

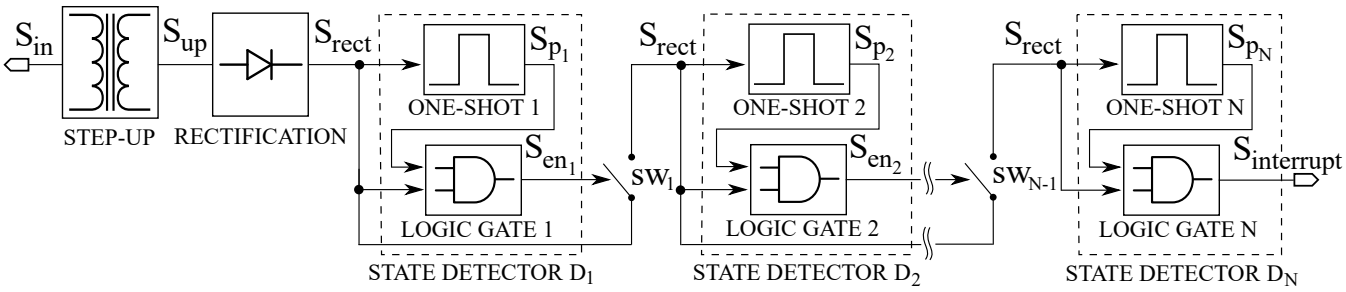


Fig. 2. Multivibrator-based WuRx block diagram.

$S_{rect}$). $S_{p_1}$ has a longer duration than that of $S_{rect}$. Next these two signals go into logic gate 1, and are compared. If $S_{rect}$ resembles the predefined WuC, logic gate 1 will enable the second state detector $D_2$ through the switch $sw_1$. $D_2$ in turn will generate a new pulse $S_{p_2}$, and compare it to $S_{rect}$. Again the comparison result is used as enabling signal of the successive state detector. Therefore the identification process consists into generating a pulse signal, and comparing it to the input one. The sensor node will be activated by the wake-up interrupt signal $S_{interrupt}$ only if all the state detectors are sequentially enabled, thus guaranteeing an identity-based wake-up. The WuRx has $N$ logic gates and multivibrators, and $N-1$ switches, since the first state detector is by default enabled. Logic gates from 1 to $N-1$ are used to drive the enabling switches, while the $N$th logic gate asserts the interrupt signal. The more complex the WuC signal, the larger the number of state detectors. An example of WuRx waveforms is depicted in Fig.3, where two state detectors are implemented, and the WuC signal is $H$-$L$-$H$. By $H$ is meant a 'high' state, i.e. $S_{in}$ (and consequently $S_{rect}$) is present at the WuRx input for a certain time window. By $L$ is meant a 'low' state, i.e. the input signal is not present at the WuRx input ($V_{in} = 0V$). During the time window $\Delta t_1$ the input signal $S_{in}$ is rectified. In response to $S_{rect}$, the multivibrator generates the pulse $S_{p_1}$ with duration $\delta\tau_1$. In order to correctly detect the 'low' state and generate the first enabling signal, logic gate 1 has to implement the logic function $S_{p_1}\&\overline{S}_{rect}$. The $\&$ symbol represents the logical conjunction operation, while the bar over $\overline{S}_{rect}$ represents the signal opposite state. Therefore since $S_{rect}$ is 'low' and $S_{p_1}$ is 'high' during $\Delta t_2$, the enabling signal $S_{en_1}$ goes 'high'. Consequently the second state detector $D_2$ is now enabled. Next $\overline{S}_{rect}$ is used to trigger the second multivibrator, thus generating a new pulse $S_{p_2}$ with duration $\delta\tau_2$. As before, the generated pulse is compared to the rectified signal, which is 'high' during the time window $\Delta t_3$. If logic gate 2 implements the logic operation $S_{p_2}\&S_{rect}$, then the interrupt signal $S_{interrupt}$ goes 'high', and the sensor node wakes up. The sensor node activation is therefore associated to a sequential verification of the WuC signal.

## III. Circuit Implementation

The proposed WuRx has been implemented with the circuit in Fig.4. The circuit configuration depends on the WuC signal.

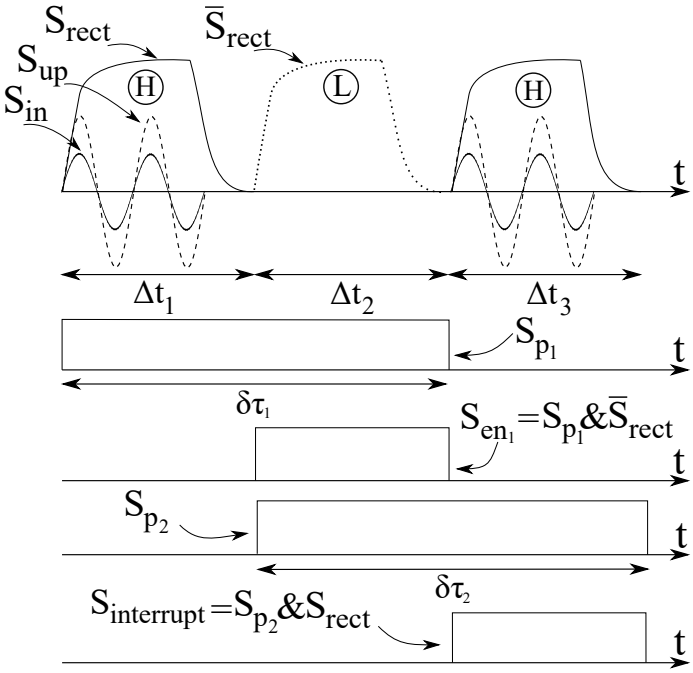


Fig. 3. WuRx waveforms when the WuC is $H$-$L$-$H$.

In this case two state detectors are considered: the first one ($D_1$) is a 'low' state detector, while $D_2$ is a 'high' one. This implies that the circuit in Fig.4 can detect the WuC signal $H$-$L$-$H$ (Fig.3). The step-up and rectification blocks are realized through a Delon circuit [28]. The resistor $R$ is used to discharge the rectified voltage.

### A. Monostable Multivibrator

The monostable multivibrator is implemented through a 2-input NOR gate ($M_{p,A,B}$, $M_{n,A,B}$), a resistor ($R_p$), a capacitor ($C_p$) and an inverter ($M_{p,inv}$, $M_{n,inv}$) [27]. Considering multivibrator 1, suppose that initially the voltage at the input of $M_{p_1,A}$ and $M_{n_1,A}$ is 'low', and the NOR gate output is 'high'. Under these assumptions, $V_{m_1}$ is 'high' because of $R_{p_1}$, and consequently the inverter output is 'low'. When a pulse is applied to the input (e.g. $V_{rect}$), $V_{m_1}$ and the NOR gate output voltage go to zero volts, and so the inverter output goes 'high'. Since the inverter output is fed back to the NOR

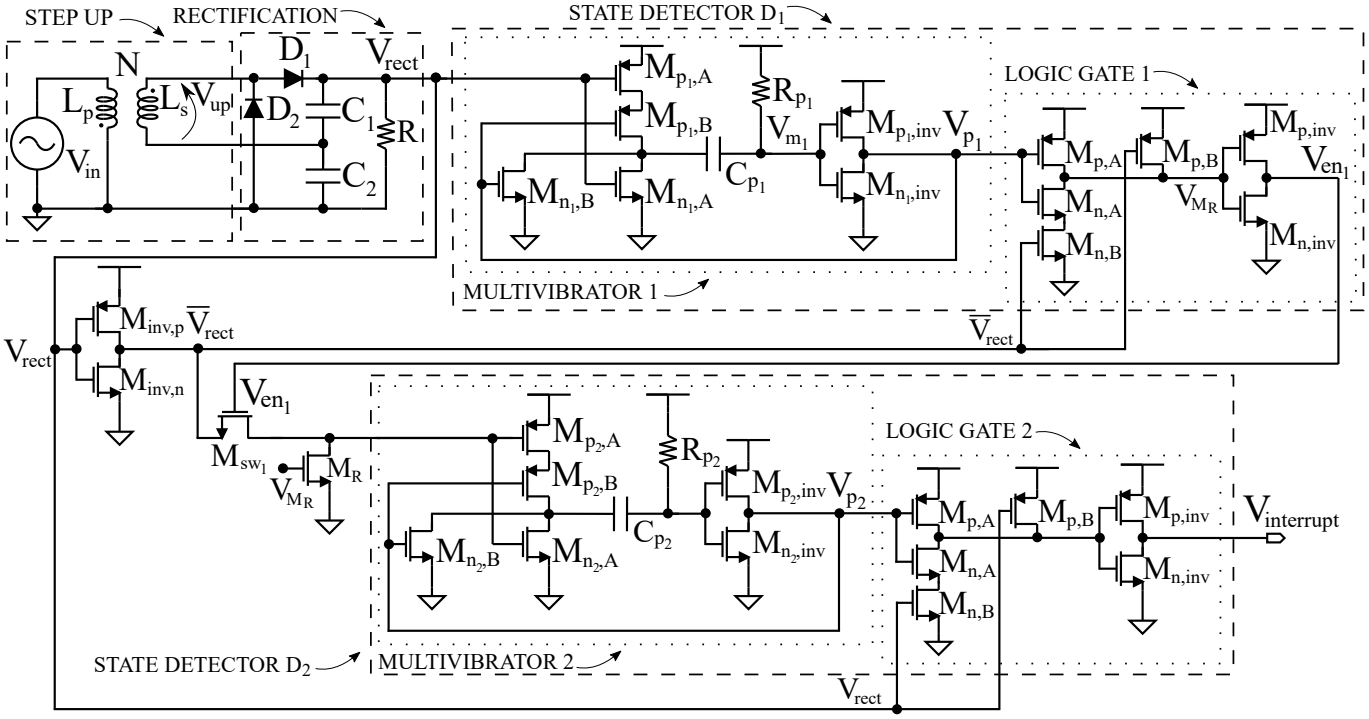


Fig. 4. Circuit implementation of the proposed WuRx, with two multivibrators and logic gates.

gate input ($M_{p_1,B}$ and $M_{n_1,B}$), the NOR gate output voltage is held at zero volts. At this point $C_{p_1}$ starts to get charged through $R_{p_1}$, so $V_{m_1}$ increases. The voltage across $C_{p_1}$ can be expressed as:

$$V_{C_{p_1}} = V_{DD}\left(1 - \exp\left(-\frac{t}{R_{p_1}C_{p_1}}\right)\right) \quad (1)$$

where $V_{DD}$ is the supply voltage. Assuming that the inverter threshold voltage $V_{th,inv}$ is $V_{DD}/2$, it follows that $C_{p_1}$ will be charged up to $V_{th,inv}$ in a time given by:

$$t = R_{p_1}C_{p_1} ln\left(\frac{V_{DD}}{V_{DD} - V_{th,inv}}\right) = R_{p_1}C_{p_1} ln(2) \quad (2)$$

from which follows that the multivibrator output pulse $V_{p_1}$ has a duration of approximately $0.7R_{p_1}C_{p_1}$ ($\delta\tau_1$ in Fig.3). As soon as the inverter gets triggered, the voltage $V_{m_1}$ goes to $V_{dd} + V_{dd}/2$. The time required to re-trigger the multivibrator is therefore dependent on the time needed to $V_{m_1}$ to decrease back to $V_{dd}$. From a process variations point of view, the multivibrator resistor and capacitor are the most critical components, since they determine the signals comparison time window.

### *B. Logic Gate*

The logic gates compare the multivibrators outputs with the rectified voltage. Logic gate 1 in Fig.4 is an AND gate realized by inverting a NAND gate. Its output ($V_{en_1}$) is 'high' when both the inputs are 'high' at the same time. So logic gate 1 drives an NMOS switch ($M_{sw_1}$). Alternatively is possible to use a NAND gate and a PMOS switch. In order to detect a 'low' state, $V_{rect}$, which is assumed to be 'low', is inverted by ($M_{inv,p}$, $M_{inv,n}$). Therefore since $V_{p_1}$ and $\overline{V}_{rect}$ are both 'high', $V_{en,1}$ is 'high' as well and enables the switch $M_{sw_1}$. In order to trigger the multivibrator of the second state detector, a 'high' voltage is required at its input. A possible solution is to use the inverted rectified voltage. Transistor $M_R$ is used to discharge the inverted rectified voltage when $M_{sw_1}$ turns off. So multivibrator 2 is triggered, and a pulse $V_{p_2}$ results at its output. Since $D_2$ is a 'high' state detector, logic gate 2 receives $V_{rect}$ at the other input, thus generating the interrupt voltage.

## IV. Simulation Results

Simulations in TSMC-180nm CMOS process were performed to verify the proposed architecture. The simulated WuRx is composed of three state detectors. $D_1$ and $D_2$ are 'low' state detectors, while $D_3$ is a 'high' state detector. Therefore the WuRx wakes up the sensor node if the WuC $H$-$L$-$L$-$H$ is received. Each state has a period $T = 1.5ms$, so a four-states WuC has a duration of $6ms$. The applied input voltage $V_{in}$ consists of pulsed sine waves, with frequency $40kHz$ and amplitude $200mV$ (Fig.5(a)). Therefore an acoustic WuRx is considered [16], [18]–[20]. The circuit simulation parameters are reported in Table I. The circuit can be tuned to operate at different frequencies, by modifying the step-up and the rectification stages. The multivibrators resistors are implemented with a cascade of two diode-connected PMOS, with unit width and length. The NOR and NAND gates are sized with minimum channel width and length, while the inverters

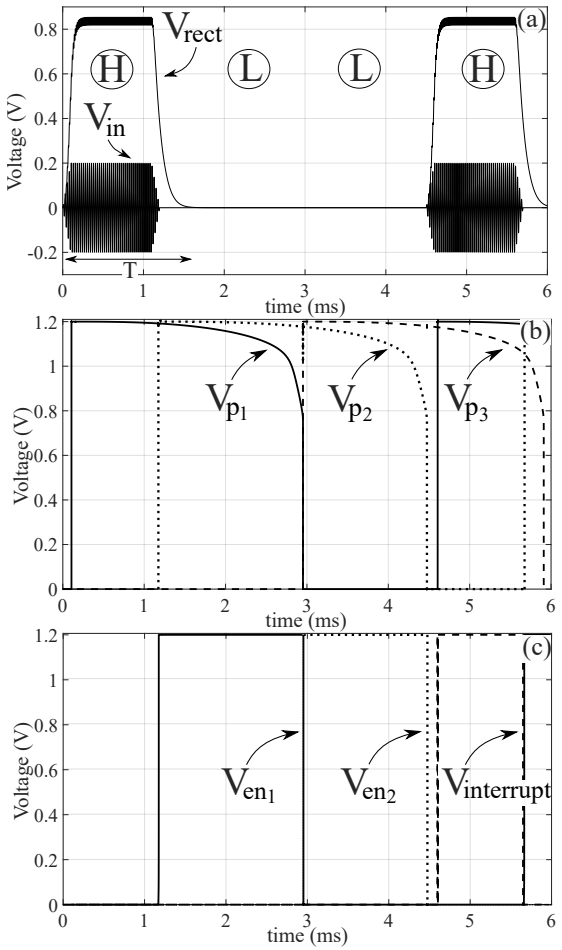


Fig. 5. WuRx simulation results: (a) $V_{in}$ and $V_{rect}$. (b) $V_{p_1}$, $V_{p_2}$ and $V_{p_3}$. (c) $V_{en_1}$, $V_{en_2}$ and $V_{interrupt}$.

have a symmetric switching point around $V_{DD}/2$, where $V_{DD}$ is equal to $1.2V$. The simulation results validated the concept. $V_{rect}$ is initially 'high' for a time window $T = 1.5ms$. So $D_1$ is triggered, and its multivibrator generates the pulse $V_{p_1}$, which stays 'high' for $3ms$ (Fig.5(b)). During the second time window ($t = 1.5ms$ to $t = 3ms$), $V_{rect}$ is 'low'. Since $D_1$ is a 'low' state detector, the enabling signal $V_{en_1}$ goes 'high' as shown in Fig.5(c). Consequently $D_2$, which is a 'low' state detector as $D_1$, is now active. As explained in Sect.III, to detect a 'low' state the inverted rectified voltage is used to trigger the second multivibrator. The latter generates the pulse $V_{p_2}$, which stays 'high' approximately for $3ms$. As before, the enabling signal $V_{en_2}$ goes 'high', thus activating $D_3$, which is a 'high' state detector. Again the inverted rectified voltage is used to trigger the successive multivibrator, which generates the pulse $V_{p_3}$ ($t = 3ms$ to $t = 6ms$). Since $V_{rect}$ is 'high' as well in the time window ($t = 4.5ms$ to $t = 6ms$), logic gate 3 finally generates $V_{interrupt}$.

### A. Power Consumption

During the detection of the WuC ($H$-$L$-$L$-$H$) the WuRx consumes $0.66\mu A$, at which corresponds an average power consumption of $0.8\mu W$. Instead in the idle mode the WuRx consumes $48.6pA$, at which corresponds an average power consumption of $58.4pW$. The power consumption in the active mode is WuC dependent, i.e. a longer WuC would imply more state detectors and therefore a higher power consumption; when detecting the WuC $H$-$L$-$L$-$H$-$L$-$H$, the WuRx consumes $1.1\mu W$. A comparison with other acoustic WuRxs is reported in Table II. The circuit is ultra-low power both in active and idle mode.

TABLE I
CIRCUIT SIMULATION PARAMETERS

| Component | Parameter | Value |
|---|---|---|
| Supply Voltage | $V_{DD}$ | $1.2V$ |
| Transformer | $L_p$ | $4\mu H$ |
| | $L_s$ | $400\mu H$ |
| Rectifier | $C_{1,2}$ | $200nF$ |
| | $R$ | $1k\Omega$ |
| Multivibrators | $C_{p_1}$ | $25pF$ |
| | $C_{p_2}$ | $29pF$ |
| | $C_{p_3}$ | $26pF$ |

TABLE II
POWER CONSUMPTION COMPARISON WITH OTHER WURXS

| $\mathbf{P_{idle}}$ | $\mathbf{P_{active}}$ | $\mathbf{f_{input}}$ | $\mathbf{V_{dd}}$ | Work |
|---|---|---|---|---|
| $58.4pW$ | $0.8\mu W$ | $40kHz$ | $1.2V$ | This |
| $3\mu W$ | $8.1\mu W$ | $85kHz$ | $3.3V$ | [19] |
| $1.64\mu W$ | $14\mu W$ | $40kHz$ | $2V$ | [18] |
| – | $4\mu W$ | $43kHz$ | $0.6V$ | [16] |
| $45\mu W$ | $420\mu W$ | $20kHz$ | $3V$ | [20] |

## V. CONCLUSIONS

In this work an ultra-low power multivibrator-based WuRx concept for wireless sensor networks is proposed. The WuRx compares the duration of the input signal to predefined pulses of fixed duration, generated by multivibrators. The system exploits the operation of complementary circuit design, such as simple logic gates, to achieve low power system operation. The input wake-up call is sequentially decoded and verified by the proposed WuRx, to generate the interrupt signal. An implementation in TSMC-180nm CMOS process is proposed and simulated, confirming the concept. The proposed implementation of the WuRx consumes $0.8\mu W$ and $58.4pW$ in the active and idle modes respectively.

## REFERENCES

[1] A. Flammini and E. Sisinni, "Wireless Sensor Networking in the Internet of Things and Cloud Computing Era," *Procedia Engineering*, vol. 87, pp. 672–679, 2014.

[2] D. Kandris, C. Nakas, D. Vomvas, and G. Koulouras, "Applications of Wireless Sensor Networks: An Up-to-Date Survey," *Applied System Innovation*, vol. 3, no. 1, p. 14, 2020.

[3] A. Al-Fuqaha, M. Guizani, M. Mohammadi, M. Aledhari, and M. Ayyash, "Internet of Things: A Survey on Enabling Technologies, Protocols, and Applications," *IEEE Communications Surveys Tutorials*, vol. 17, no. 4, pp. 2347–2376, 2015.

[4] G. Anastasi, M. Conti, M. Di Francesco, and A. Passarella, "Energy conservation in wireless sensor networks: A survey," *Ad hoc networks*, vol. 7, no. 3, pp. 537–568, 2009.

[5] I. Demirkol, C. Ersoy, and E. Onur, "Wake-up receivers for wireless sensor networks: benefits and challenges," *IEEE Wireless Communications*, vol. 16, no. 4, pp. 88–96, 2009.

[6] E.-Y. A. Lin, J. M. Rabaey, and A. Wolisz, "Power-efficient rendezvous schemes for dense wireless sensor networks," in *2004 IEEE International Conference on Communications (IEEE Cat. No.04CH37577)*, vol. 7, 2004, pp. 3769–3776 Vol.7.

[7] A. Rasul and T. Erlebach, "Reducing Idle Listening during Data Collection in Wireless Sensor Networks," in *2014 10th International Conference on Mobile Ad-hoc and Sensor Networks*, 2014, pp. 16–23.

[8] D. Ghose, F. Y. Li, and V. Pla, "MAC Protocols for Wake-Up Radio: Principles, Modeling and Performance analysis," *IEEE Transactions on Industrial Informatics*, vol. 14, no. 5, pp. 2294–2306, 2018.

[9] J. Oller, I. Demirkol, J. Casademont, J. Paradells, G. U. Gamm, and L. Reindl, "Has Time Come to Switch From Duty-Cycled MAC Protocols to Wake-Up Radio for Wireless Sensor Networks?" *IEEE/ACM Transactions on Networking*, vol. 24, no. 2, pp. 674–687, 2016.

[10] R. Piyare, A. L. Murphy, C. Kiraly, P. Tosato, and D. Brunelli, "Ultra Low Power Wake-Up Radios: A Hardware and Networking Survey," *IEEE Communications Surveys Tutorials*, vol. 19, no. 4, pp. 2117–2157, 2017.

[11] D. Galante-Sempere, D. Ramos-Valido, S. Lalchand Khemchandani, and J. Del Pino, "Low-Power RFED Wake-Up Receiver Design for Low-Cost Wireless Sensor Network Applications," *Sensors*, vol. 20, no. 22, p. 6406, 2020.

[12] D. D. Wentzloff, A. Alghaihab, and J. Im, "Ultra-Low Power Receivers for IoT Applications: A Review," in *2020 IEEE Custom Integrated Circuits Conference (CICC)*. IEEE, 2020, pp. 1–8.

[13] J. Moody, P. Bassirian, A. Roy, N. Liu, N. S. Barker, B. H. Calhoun, and S. M. Bowers, "Interference Robust Detector-First Near-Zero Power Wake-Up Receiver," *IEEE Journal of Solid-State Circuits*, vol. 54, no. 8, pp. 2149–2162, 2019.

[14] S. Koeble, S. Heller, and P. Woias, "A narrow-band and ultra-low-power 433 MHz wake-up receiver," in *Journal of Physics: Conference Series*, vol. 1407, no. 1. IOP Publishing, 2019, p. 012093.

[15] T. Ma, "A Bit Sampled Wake-Up Receiver with Logarithmic Detector Architecture," in *2017 International Conference on Cyber-Enabled Distributed Computing and Knowledge Discovery (CyberC)*. IEEE, 2017, pp. 445–449.

[16] K. Yadav, I. Kymissis, and P. R. Kinget, "A 4.4uW wake-up receiver using ultrasound data communications," in *2011 Symposium on VLSI Circuits - Digest of Technical Papers*, 2011, pp. 212–213.

[17] Y. C. Wong, S. H. Tan, R. S. S. Singh, H. Zhang, A. Syafeeza, and N. Hamid, "Low power wake-up receiver based on ultrasound communication for wireless sensor network," *Bulletin of Electrical Engineering and Informatics*, vol. 9, no. 1, pp. 21–29, 2020.

[18] E. Lattanzi, M. Dromedari, V. Freschi, and A. Bogliolo, "A sub-μA ultrasonic wake-up trigger with addressing capability for wireless sensor nodes," *International Scholarly Research Notices*, vol. 2013, 2013.

[19] A. Sánchez, S. Blanc, P. Yuste, A. Perles, and J. J. Serrano, "An Ultra-Low Power and Flexible Acoustic Modem Design to Develop Energy-Efficient Underwater Sensor Networks," *Sensors*, vol. 12, no. 6, pp. 6837–6856, 2012.

[20] A. Bannoura, F. Höflinger, O. Gorgies, G. U. Gamm, J. Albesa, and L. M. Reindl, "Acoustic Wake-Up Receivers for Home Automation Control Applications," *Electronics*, vol. 5, no. 1, p. 4, 2016.

[21] H. Fuketa, S. O'uchi, and T. Matsukawa, "A 0.3-V 1-μW Super-Regenerative Ultrasound Wake-Up Receiver With Power Scalability," *IEEE Transactions on Circuits and Systems II: Express Briefs*, vol. 64, no. 9, pp. 1027–1031, 2016.

[22] F. Höflinger, G. U. Gamm, J. Albesa, and L. M. Reindl, "Smartphone remote control for home automation applications based on acoustic wake-up receivers," in *2014 IEEE International Instrumentation and Measurement Technology Conference (I2MTC) Proceedings*. IEEE, 2014, pp. 1580–1583.

[23] J. Chen, Z. Dai, and Z. Chen, "Development of Radio-Frequency Sensor Wake-Up with Unmanned Aerial Vehicles as an Aerial Gateway," *Sensors*, vol. 19, no. 5, p. 1047, 2019.

[24] U. Dudko and L. Overmeyer, "Optical Wake-Up From Power-Off State for Autonomous Sensor Nodes," *IEEE Sensors Journal*, vol. 21, no. 3, pp. 3225–3232, 2021.

[25] G. Kim, Y. Lee, S. Bang, I. Lee, Y. Kim, D. Sylvester, and D. Blaauw, "A 695 pW standby power optical wake-up receiver for wireless sensor nodes," in *Proceedings of the IEEE 2012 Custom Integrated Circuits Conference*. IEEE, 2012, pp. 1–4.

[26] W. Lim, T. Jang, I. Lee, H.-S. Kim, D. Sylvester, and D. Blaauw, "A 380pW Dual Mode Optical Wake-up Receiver with Ambient Noise Cancellation," in *2016 IEEE Symposium on VLSI Circuits (VLSI-Circuits)*. IEEE, 2016, pp. 1–2.

[27] R. J. Baker, *CMOS: Circuit Design, Layout, and Simulation*. John Wiley & Sons, 2019, ch. 18, pp. 539–540.

[28] A. Mouapi, N. Hakem, and N. Kandil, "Performances Comparison of Shottky Voltage Doubler Rectifier to support RF Energy Harvesting," in *2020 IEEE International Conference on Environment and Electrical Engineering and 2020 IEEE Industrial and Commercial Power Systems Europe (EEEIC / I&CPS Europe)*, 2020, pp. 1–5.